

Structural Basis for Distinct Oncogenic Activities of *Helicobacter pylori* CagA Variants

Helicobacter pylori CagA undergoes tyrosine-phosphorylation to interact with the pro-oncogenic phosphatase SHP2 and thereby triggers gastric carcinogenesis. Here we determined the crystal structure of the CagA-SHP2 binding interface. Structure-function analysis revealed that East Asian-specific CagA exploits a characteristic Phe residue present at the phosphotyrosine+5 position to achieve binding to SHP2 with more than 100-fold greater affinity compared to the world-standard CagA, which contains Asp residue at the equivalent position. Small-angle X-ray scattering also demonstrated the conformational change of activated SHP2 upon CagA-binding in solution. The present study clarified the structural mechanism underlying the highest incidence of gastric cancer in East Asia.

Chronic infection with *Helicobacter pylori* is etiologically linked to the development of gastric cancer [1-2], which occurs most frequently in East Asian countries. *H. pylori* CagA protein is known to play a pivotal role in gastric carcinogenesis. Notably, East Asian CagA, a CagA subtype produced by *H. pylori* endemically circulating in East Asia, is epidemiologically associated with gastric cancer more intimately compared to Western CagA, a standard CagA species found in the rest of the world except East Asia [3]. CagA is injected into gastric epithelial cells, where it undergoes tyrosine-phosphorylation on multiple Glu-Pro-Ile-Tyr-Ala (EPIYA) motifs in the structurally disordered C-terminal portion [4]. The sequences flanking EPIYA have defined EPIYA-A, -B, -C and -D segments, each of which is composed of 30–45 residues containing a single EPIYA motif. Whereas most CagA subtypes commonly contain EPIYA-A and -B segments, EPIYA-C segment is present in Western CagA and absent in East Asian CagA, which is instead characterized by the presence of EPIYA-D segment [3, 5]. Upon tyrosine-phosphorylation on EPIYA-C or EPIYA-D segment, CagA specifically interacts with SHP2, a pro-oncogenic phosphatase containing N-terminal tandem SH2 (N-SH2 and C-SH2) and C-terminal catalytic domains [6]. The SHP2-binding capacity of CagA is

involved in its oncogenic activity *in vitro* and *in vivo* [7, 8], indicating that CagA-mediated SHP2 deregulation acts as a driving force in gastric carcinogenesis. To elucidate the mechanism underlying the distinct biological activities of the geographical CagA variants, structural and biochemical analyses of CagA-SHP2 complexes were performed [9].

We determined crystal structures of tandem SH2 domains isolated from SHP2 complexed with tyrosine-phosphorylated EPIYA-D peptide (EPIpYA-D: ASPEPIpYATIDFD) or EPIYA-C peptide (EPIpYA-C: VSPEPIpYATIDDL) [Fig. 1(A)]. The co-crystal structure revealed that the aromatic side chain of the Phe located at the pY+5 position in EPIYA-D was sticking inwards, making significant contact with a cryptic hollow present on the ligand-binding floor of the N-SH2 surface, where a π - π interaction can be observed between the phenyl group of the Phe residue and the peptide bond connecting Gly-67 and Gly-68 in the N-SH2 domain [Fig. 1(B)]. In contrast, no such structure was observed in the tandem SH2 complexed with EPIpYA-C, which has acidic Asp residue at the pY+5 position. Surface plasmon resonance analysis further demonstrated that the monovalent interaction of EPIpYA-D with the SHP2 N-SH2 domain ($K_D = 0.185 \mu\text{M}$) showed ~120-fold

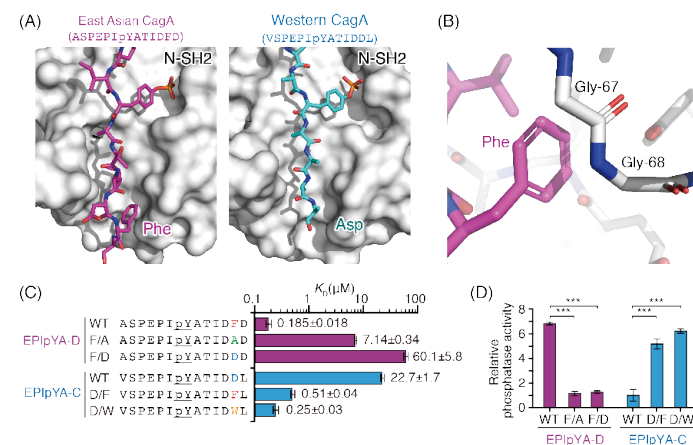


Figure 1: Structures and biochemical properties of CagA-SHP2 interaction. (A) Crystal structures of tandem SH2 domains of SHP2 complexed with EPIpYA-D (left, PDB ID: 5X94) or EPIpYA-C (right, PDB ID: 5X7B). The views focus on the N-SH2/peptide interface. (B) Possible π - π interaction between the Phe residue specifically present in EPIpYA-D and the peptide bond connecting Gly-67 and Gly-68 in N-SH2. (C) Dissociation constants for the interaction of a series of CagA peptides with N-SH2 were measured by surface plasmon resonance analysis. Residues at the pY+5 position are highlighted with distinct colors. (D) Phosphatase activities of SHP2 in the presence of CagA peptides were examined by measuring the hydrolysis rate of *p*-nitrophenylphosphate.

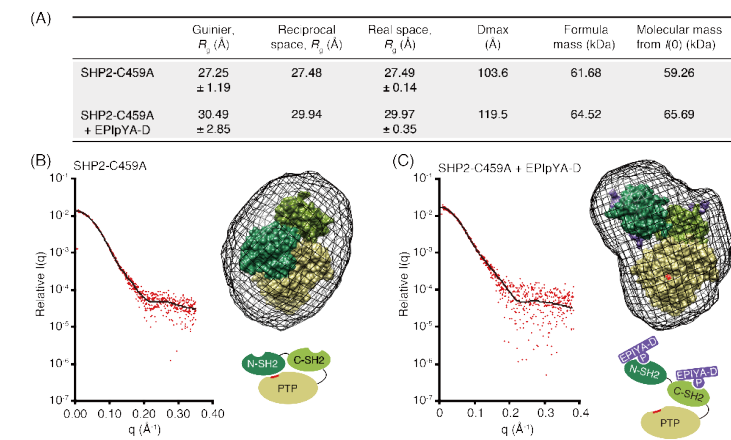


Figure 2: SAXS analysis of SHP2-C459A complexed with EPIpYA-D. (A) Summary of structural parameters. (B) SAXS data of peptide-free SHP2 was evaluated by the CRYSOLOG program (left), and the calculated surface and envelope models were obtained (top right). Schematic for the closed inactive form of SHP2 is shown (bottom right). (C) SAXS data of SHP2 complexed with EPIpYA-D was refined by the CORAL program (left), and the calculated surface and envelope models were obtained (top right). Schematic for the open active form of SHP2 upon EPIpYA-D binding is shown (bottom right). The exposed catalytic center in the phosphatase (PTP) domain is indicated in red. This figure was prepared by modifying the original article [9], the copyright of which is owned by the authors.

greater affinity than that of EPIpYA-C ($K_D = 22.7 \mu\text{M}$) [Fig. 1(C)]. Phe-to-Asp and Phe-to-Ala substitutions at the pY+5 position in EPIpYA-D resulted in drastic reduction in the SHP2 interaction. Reciprocally, Asp-to-Phe and Asp-to-Trp substitutions at the pY+5 position in EPIpYA-C significantly promoted the binding capacity. These data consolidate the functional relevance for the binding structure of the aromatic Phe residue in EPIpYA-D. CagA also directly stimulated SHP2 activity [Fig. 1(D)] and thereby enhanced the neoplastic trait of gastric epithelial cells in a binding affinity-dependent manner. Collectively, the Phe residue at the pY+5 position in EPIYA-D segment acts as a barb that stabilizes the CagA-SHP2 complex, whereas barbless EPIpYA-C easily dissociates from the N-SH2 domain. Of note, we also found that tandem duplication of EPIYA-C segment in a single molecule, which is a characteristic of cancer-associated Western CagA, enables high-avidity divalent interactions with N-SH2 and C-SH2.

To investigate the structural alteration during SHP2 activation, we performed small-angle X-ray scattering (SAXS) analysis (Fig. 2). Scattering profiles of SHP2 with mutation at the catalytic center (C459A) were obtained in the presence and absence of the EPIpYA-D peptide. Peptide-free SHP2 indicated a radius of gyration R_g (Guinier) of 27.25 Å and a maximum dimension D_{max} of 103.6 Å [Fig. 2(A)] and fitted well with the calculated profile of the previously-reported crystal structure of the inactive form of SHP2 (PDB ID: 2SHP) with a χ value of 1.107 [Fig. 2(B)]. In the presence of EPIpYA-D, R_g (Guinier) and D_{max} were expanded to 30.49 Å and 119.5 Å, respectively. Rigid body modeling based on the scattering profile of the peptide-bound SHP2 provided an open conformation of SHP2, in which the EPIpYA-D-bound N-SH2 domain is dissociated from the phosphatase domain, resulting in enzymatic activation with exposure of the catalytic center [Fig. 2(C)]. Muta-

tional analysis also revealed that binding of EPIpYA-D to the N-SH2 domain but not to the C-SH2 domain is required for the structural alteration of SHP2.

The present study demonstrates the structural basis for the functional impact of the single amino-acid polymorphism in CagA and clarifies the cancer-predisposing mechanisms of SHP2 activation that are differentially achieved by two major oncogenic CagA isoforms.

REFERENCES

- [1] J. Parsonnet, G. D. Friedman, N. Orentreich and H. Vogelman, *Gut* **40**, 297 (1997).
- [2] M. J. Blaser, G. I. Perez-Perez, H. Kleanthous, T. L. Cover, R. M. Peek, P. H. Chyou, G. N. Stemmermann and A. Nomura, *Cancer Res.* **55**, 2111 (1995).
- [3] M. Hatakeyama, *Nat. Rev. Cancer* **4**, 688 (2004).
- [4] T. Hayashi, M. Senda, H. Morohashi, H. Higashi, M. Horio, Y. Kashiba, L. Nagase, D. Sasaya, T. Shimizu, N. Venugopalan, H. Kumeta, N. N. Noda, F. Inagaki, T. Senda and M. Hatakeyama, *Cell Host Microbe* **12**, 20 (2012).
- [5] H. Higashi, R. Tsutsumi, A. Fujita, S. Yamazaki, M. Asaka, T. Azuma and M. Hatakeyama, *Proc. Natl. Acad. Sci. U.S.A.* **99**, 14428 (2002).
- [6] H. Higashi, R. Tsutsumi, S. Muto, T. Sugiyama, T. Azuma, M. Asaka and M. Hatakeyama, *Science*, **295**, 683 (2002).
- [7] N. Ohnishi, H. Yuasa, S. Tanaka, H. Sawa, M. Miura, A. Matsui, H. Higashi, M. Musashi, K. Iwabuchi, M. Suzuki, G. Yamada, T. Azuma and M. Hatakeyama, *Proc. Natl. Acad. Sci. U.S.A.* **105**, 1003 (2008).
- [8] L. Nagase, T. Hayashi, T. Senda and M. Hatakeyama, *Sci. Rep.* **5**, 15749 (2015).
- [9] T. Hayashi, M. Senda, N. Suzuki, H. Nishikawa, C. Ben, C. Tang, L. Nagase, K. Inoue, T. Senda and M. Hatakeyama, *Cell Reports* **20**, 2876 (2017).

BEAMLINES

BL-10C, BL-17A and BL-5A

T. Hayashi¹, M. Senda², N. Suzuki², T. Senda² and M. Hatakeyama¹ (¹The Univ. of Tokyo, ²KEK-IMSS-PF/SBRC)